Research paper

Fluorinated captopril analogues inhibit metallo-β-lactamases and facilitate structure determination of NDM-1 binding pose

Alexandra Kondratieva [a], Katarzyna Palica [b], Christopher Frøhlich [c], Rebekka Rolfsnes Hovd [d], Hanna-Kirsti S. Leiros [a], Mate Erdelyi [b], Annette Bayer [a,*]

[a] Department of Chemistry, UiT The Arctic University of Norway, NO-9037, Tromsø, Norway
[b] Department of Chemistry – BMC, Organic Chemistry, Uppsala University, 752 37, Uppsala, Sweden
[c] Department of Pharmacy, UiT The Arctic University of Norway, NO-9037, Tromsø, Norway
[d] AdjuTec Pharma, NO-0165 Oslo, Norway

ABSTRACT

Bacterial resistance to the majority of clinically used β-lactam antibiotics is a global health threat and, consequently, the driving force for the development of metallo-β-lactamase (MBL) inhibitors. The rapid evolution of new MBLs calls for new strategies and tools for inhibitor development. In this study, we designed and developed a series of trifluoromethylated captopril analogues as probes for structural studies of enzyme-inhibitor binding. The new compounds showed activity comparable to the non-fluorinated inhibitors against the New Delhi Metallo-β-lactamase-1 (NDM-1). The most active compound, a derivative of D-captopril, exhibited an IC_{50} value of 0.3 μM. Several compounds demonstrated synergistic effects, restoring the effect of meropenem and reducing the minimum inhibitory concentration (MIC) values in NDM-1 (up to 64-fold), VIM-2 (up to 8-fold) and IMP-26 (up to 8-fold) harbouring *Escherichia coli*. NMR spectroscopy and molecular docking of one representative inhibitor determined the binding pose in NDM-1, demonstrating that fluorinated analogues of inhibitors are a valuable tool for structural studies of MBL-inhibitor complexes.

1. Introduction

Antimicrobial resistance presents a worldwide challenge to global health, threatening the effective treatment of an increasing range of infections as well as holding back advances in medicine and drug development [1]. Although there are several mechanisms through which bacterial resistance to β-lactam antibiotics arises, the production of β-lactamase enzymes is considered the most common and worrying in Gram-negative pathogens [2]. These enzymes mediate the hydrolysis of the β-lactam ring, which deactivates penicillins, cephalosporins and even carbapenems, the so-called last-resort antibiotics.

β-Lactamases can be divided into two main groups, based on the mechanism of hydrolysis: serine β-lactamases (SBLs) and metallo-β-lactamases (MBLs) [3]. SBLs constitute Ambler classes A, C and D and bind covalently to a β-lactam antibiotic via a nucleophilic serine moiety. Ambler class B, or MBLs, rely on zinc ions in the active site to activate a water molecule for the cleavage of the β-lactam ring. At present (December 2023), around 940 MBLs have been identified according to the Beta Lactamase Database (BLDB, http://www.bldb.eu/), whereof

around 600 belong to the B1 subgroup [4]. The B1 subgroup contains the clinically most relevant MBLs, such as New Dehli metallo-β-lactamases (NDMs), Verona integron-encoded metallo-β-lactamases (VIMs) and imipenemases (IMPs) [5]. Many B1 MBLs are structurally diverse due to their low sequence identity [5b], e.g. the sequence identity of NDM-1 and IMP-26 is 34 %.

One way to oppose the resistance caused by β-lactamases is the development of small molecule β-lactamase inhibitors to be administered together with the antibiotic. While SBLs are inhibited by a variety of clinically approved inhibitors such as tazobactam, avibactam and relebactam [6], there are none available for MBLs [7]. Currently three dual SBL/MBL inhibitors: VNRX-5133 (taniborbactam), QPX7728 (xeruborbactam) and QPX7831 are under evaluation in clinical studies [8], hopefully leading to the first clinically approved MBL inhibitor after over 30 years of research [9]. However, due to the continuous evolution of MBL enzymes and their structural diversity, new inhibitors as well as new strategies for inhibitor development are needed.

Thiols are a compound class known to broadly inhibit MBLs due to the ability of sulfur to coordinate zinc, thus a number of thiol-based

---

inhibitors have been reported [10]. (2S)-1-((2S)-2-methyl-3-sulfanyl-propanoyl)pyrrolidine-2-carboxylic acid, more commonly known as L-captopril (Fig. 1), is a thiol-containing molecule developed to target the angiotensin-converting enzyme (ACE) and is a clinically approved drug used for controlling high blood pressure [11]. It has been shown that L-captopril (the (2S,2′S)-stereoisomer), as well as its three stereoisomers, could be of interest for the development of new MBL inhibitors [12]. Initially, clinically used L-captopril was reported to be less active than D-captopril (the (2R,2′S)-stereoisomer) against some MBLs [14]. However, L-captopril has lately been shown to be of similar effectivity against NDM-1, with half maximal inhibitory concentration (IC$_{50}$) values in the low micromolar region [15]. Based on these findings, several captopril analogues have been developed that exhibit inhibitory activity against MBLs (Fig. 1) [13].

The development of thiol-based inhibitors has been limited by their tendency to oxidize to the corresponding disulfides, thus losing zinc binding and MBL inhibitory properties [16]. Recent attempts to overcome this limitation have focused on the development of prodrugs that release the thiol inhibitor directly in the cell. However, so far, prodrugs designed for the release of aliphatic thiol inhibitors were shown to cleave the inhibitor very slowly or not at all due to the poor leaving group ability of the aliphatic thiols [17]. Thus, structurally more diverse thiol-based inhibitors are necessary. The bioisostere replacement of H to F to manage properties of drug candidates such as bioactivity, membrane permeability, and pKa of proximal functionalities is well established [18]. However, to our knowledge, fluorinated aliphatic thiols such as trifluoromethylated captopril analogues have only been studied as ACE inhibitors [19].

The development of broad-spectrum MBL inhibitors has been strongly dependent on understanding of the binding site and binding mode. The primary source of structural information on enzyme-inhibitor complexes has been X-ray crystallography. However, according to the BLDB (status December 2023) [4], for the approximately 600 reported B1 MBLs, crystal structures of less than 10 % (40 structures) have been deposited, and even fewer of enzyme-inhibitor complexes. Solution-state NMR can serve as an alternative and provide structural insights, as demonstrated recently in the investigation of the active sites of NDM-1 and VIM-2 [20]. However, signal overlaps in the ¹H NMR dimension remain a serious challenge [21].

As native proteins lack fluorine atoms, fluorine labelling of potent MBL-inhibitors is expected to provide valuable probes for studying inhibitor binding poses, in particular when X-ray crystallography is not feasible, and when standard NMR experiments do not provide sufficient information. The ¹⁹F NMR signal of fluorine-labelled ligands provides a highly sensitive handle to locate the binding site and binding mode using 3D HOESY-HSQC (¹H,¹⁹F,¹³C). ¹⁹F NMR has a wider chemical shift scale (800 ppm) compared to ¹H NMR (15 ppm) and, consequently, ¹⁹F NMR chemical shift changes induced by binding are more pronounced and hence easier to detect. The use of ¹⁹F NMR diminishes the risk of overlaps between the signals of the protein and the binding ligand. The ¹⁹F-labelling of drug candidates [22] or of the target protein [23] has accordingly been shown to facilitate the determination of the protein-ligand binding pose as well as the mechanism of enzyme-inhibition.

We aimed for fluorinated MBL inhibitors as probes for solution-state NMR studies of MBLs as an alternative to crystallography. In this study, we describe the design and synthesis of a series of fluorinated thiol inhibitors and demonstrate their inhibitory activity against a panel of structurally diverse B1 MBLs (NDM-1, VIM-2 and IMP-26). Finally, solution-state NMR spectroscopy directed molecular docking is used to identify the binding pose of a fluorinated inhibitor with NDM-1.

2. Results and discussion

2.1. Design and synthesis

Starting from the structure of captopril (Fig. 1), we aimed to obtain compounds with the general structure **5** (Scheme 1). From a synthetic point of view, it was most feasible to expand the compound library by varying the amine part of the molecule (R′), while having a fixed fluorinated scaffold. We envisioned trifluoromethylation in the α- or β-position of the 3-mercaptopropionamide substructure of captopril as the fluorinated scaffold. By changing the position of the CF$_3$ moiety, we intended to study the effect on inhibitory activity as well as its influence on the stability of the thiol moiety towards oxidation. Direct captopril analogues of all four stereoisomers with methyl replaced by a trifluoromethyl group were synthesized. Moreover, we modified the amine part of the scaffold, inspired by previously reported compounds [13b,c].

The synthetic route towards trifluoromethyl-containing mercaptopropionamide derivatives is shown in Scheme 1. Starting with the commercially available regioisomers 2-(trifluoromethyl)acrylic acid (**1α**) or (E)-4,4,4-trifluorobut-2-enoic acid (**1β**) and thioacetic acid, compounds **2α** and **2β** were prepared according to published procedures [24]. The next step was envisioned to be a coupling reaction between the obtained acids and different amines to obtain a diverse library of fluorinated mercaptopropionamide derivatives. Using **2α** or **2β**, the corresponding amines and EDC as the coupling reagent, compounds **4αA**, **4βA** and **4αB** were obtained. No product formation was observed for coupling of **2α** or **2β** to aliphatic amines, even when using other coupling reagents and conditions. The order of the synthetic steps was therefore reversed for the remaining desired compounds.

Starting with the acrylic acids **1α** or **1β**, amide coupling was performed with various amines, followed by conjugate addition of thioacetic acid to the previously obtained amides. This approach afforded compounds **4α(C-G)** and **4β(B–H)**. For compounds with a β-CF$_3$ group, previously reported reaction conditions using HBTU as the coupling reagent and DIPEA as the base [13c] were successful, providing compounds **3βC**, **3βD**, **3βF** and **3βG** in moderate to excellent yields (45–91 %). For compounds containing an α-CF$_3$ group, the same conditions proved to be unsuccessful, resulting in mixtures of the desired product and a compound with two amines attached, according to MS. This is presumably the product of a conjugate addition of the amine to the desired α,β-unsaturated amide. The two products had similar R$_f$ values, which hampered purification by flash column chromatography. However, we discovered that using propanephosphonic acid anhydride (T3P) as the coupling reagent did not lead to formation of the problematic side-product. Further coupling reactions were carried out using T3P, affording compounds **3αC**, **3αD**, **3αE**, **3βE**, **3αF**, **3αG**, **3βH** and **3βB** in low to very good yields (30–85 %). It is noteworthy that **3C**, **3D** and **3E** were obtained as a mixture of rotamers. The conjugate addition step with thioacetic acid for α–CF$_3$–containing compounds proceeded overnight at ambient temperature, while for derivatives with a β-CF$_3$ group 60 h reaction time at 60 °C was necessary.

Compounds **4C**, **4D** and **4E** were acquired as diastereomeric mixtures, which were difficult to separate using column chromatography. For **4αD**, the separation of diastereomers using medium pressure liquid
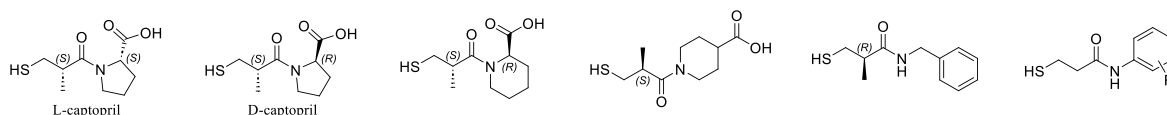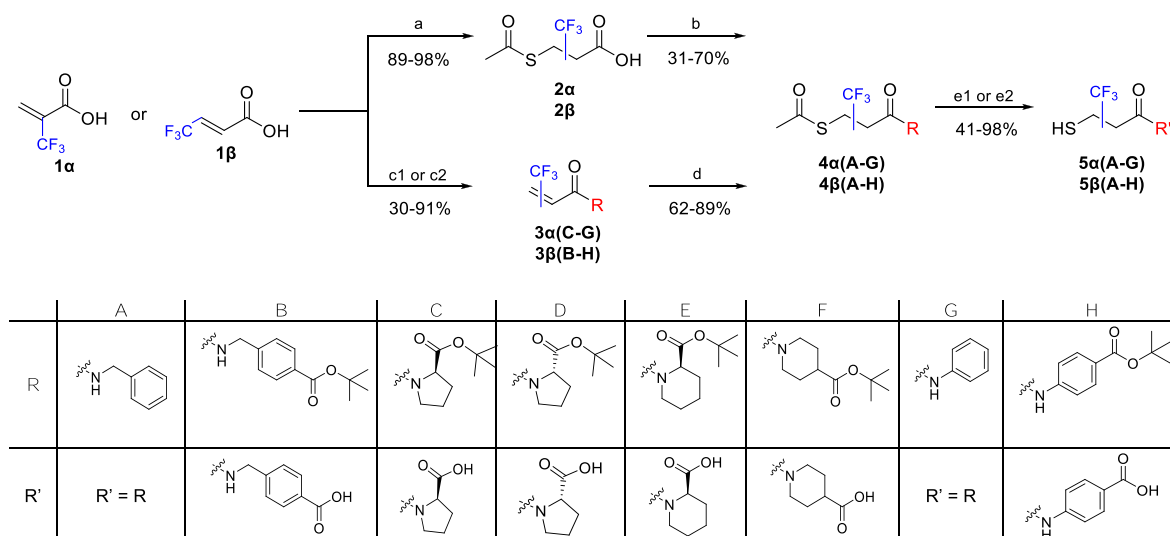

Fig. 1. D- and L-captopril and some structurally related thiol derivatives reported in literature [13] as potential MBL inhibitors.

Scheme 1. Synthetic strategy towards thiols **5α(A-G)** and **5β(A-H)**. Reaction conditions: (a) AcSH, neat, room temperature (r.t.), overnight (o.n.) or 60 °C, 60 h; (b) R–H, EDC·HCl, HOBt, *N*-methylmorpholine, DCM, 0 °C to r.t., o.n.; (c1) amine, HBTU, DIPEA or T3P, Et_3N, DCM, 0 °C to r.t., 1–4 h; (c2) amine, T3P, DIPEA, EtOAc, 0 °C to r.t., o.n.; (d) AcSH, THF, r.t., o.n. or 60 °C, 60 h; (e1) NaSMe, MeOH, −20 °C, 30 min; (e2) TFA, DCM, 50 °C, o.n. and NH_3 (aq), r.t., 3 h.

chromatography (MPLC) has previously been reported as well as the assignment of stereocenters using X-ray crystallography [19a]. Based on this data, we were able to separate the diastereomers and determine the configuration of the stereoisomers of **4αD** as well as **4αC**. For the rest of the derivatives, the diastereomers were not separated, and they were further used and analyzed as mixtures.

The last step of the synthesis was the deprotection of the thiol and, where relevant, acid moieties. For compounds requiring only a thiol deprotection (**4αA**, **4βA**, **4αG**, **4βG**), an adapted previously established procedure [25], employing sodium thiomethoxide, was used. For the rest of the derivatives, ester hydrolysis was accomplished using trifluoroacetic acid (TFA) in methylene chloride at 50 °C overnight. Subsequent removal of the acetate by treatment with aqueous ammonia for 3 h at room temperature afforded compounds **5B–F** and **5H** [26]. Compounds **5B**, **5G** and **5H** precipitated upon using the standard work-up procedure and were used for analysis without further purification. Use of normal phase column chromatography for some of the final compounds led to oxidation of the thiol moieties, resulting in disulfide formation. Primary thiols have been shown to exhibit relatively short half-lives and form disulfides faster than secondary, thus hindering synthesis and analysis [16b]. Following the same trend, compounds with an α-CF₃ group were noticeably more prone to oxidation than β-CF₃ derivatives, which complicates purification and storage of these compounds. To limit formation of the undesired disulfides, the final compounds were all purified by preparative reversed-phase HPLC. The final compounds **5α(A-G)** and **5β(A-H)** were obtained in moderate to excellent yields (41–98 %).

2.2. Inhibitory activities

The inhibitory activity of all final compounds (**5α(A-G)** and **5β(A-H)**) against NDM-1 was evaluated in an enzyme assay in terms of their half maximal inhibitory concentration (IC_{50}) values (Table 1), measured using meropenem as the reporter substrate. Initial rates of the reactions with various concentrations of the inhibitors in a 2-fold dilution series were measured and the IC_{50} values were derived from the fitted dose-response curves. To validate our assay, commercially available L-captopril was included in our compound library. The reported IC_{50} values for L-captopril vary from 9.4 to 157.4 μM [14,15], with the spread of the values being attributed to differences in assay buffers, reporter substrates and protein constructs. We obtained an IC_{50} value of 7 μM, which is in good agreement with previous reports.

The tested compounds **5α(A-G)** and **5β(A-H)** showed IC_{50} values ranging from 0.3 to >300 μM. Interestingly, the position of the CF₃ group plays a vital role in the activity of the studied inhibitors. In all cases, the compounds with an α-CF₃ group showed lower IC_{50} values than the respective β-CF₃ derivative. Furthermore, compounds containing a β-CF₃ group exhibited no significant inhibitory activity (IC_{50} >300 μM), with the exception of **5βE** (IC_{50} = 145 μM) and **5βH** (IC_{50} = 5.6 μM). It has been previously shown that a carboxylic acid moiety may be important for binding to the active site of NDM-1 [13b]. This hypothesis is corroborated by the activity of compounds **5βG** (IC_{50} = 22 μM) and **5βH** (IC_{50} = 5.6 μM), yet is contradicted by the deterioration of activity of **5αA** (IC_{50} = 20 μM) upon carboxylation (**5αB**, IC_{50} = 65 μM). This may be due to the inhibitor becoming too large to be accommodated by the active site with this modification. For piperidine-based derivatives **5αF** (IC_{50} = 2.2 μM) and **5αE** (IC_{50} = 3.2 μM), the position of the carboxylic acid has little influence on the activity.

Brem et al. carried out a study of the inhibitory activity of the four captopril stereoisomers (Fig. 2) against several MBLs, including NDM-1 [14a]. They showed that D-captopril (IC_{50} = 22 μM) was the most potent of the four possible captopril stereoisomers, followed by *epi*-D-captopril, L-captopril and *epi*-L-captopril with IC_{50} values of 64, 157 and >500 μM, respectively. In general, captopril derivatives containing the D-proline motif (*2R* configuration) showed better inhibition than those derived from L-proline (*2S* configuration). In the current study, the same trend can be seen for the trifluoromethyl-containing analogues: (2R,2′R)-**5αC** (IC_{50} = 0.3 μM), (2R,2′S)-**5αC** (IC_{50} = 4.5 μM), (2S,2′R)-**5αD** (IC_{50} = 6.1 μM), and (2S,2′S)-**5αD** (IC_{50} = 60 μM). Comparing L-captopril and its trifluoromethyl-derivative ((2S,2′R)-**5αD**), the inhibitory activity seems unaffected by the structural modification of the methyl group (IC_{50} values of 7 and 6 μM, respectively). For other compounds, replacement of the CH₃ group with a CF₃ group provided IC_{50} values in a similar range to those reported for the non-fluorinated inhibitors (Table 1, entries 3, 4, 8, 9, 12, 15, 17), but a direct comparison is challenging due to different assay conditions.

Additionally, a selection of inhibitors was tested for synergistic activity with meropenem in an NDM-1-producing *Escherichia coli* (Fig. S3, Supporting Information). The production of NDM-1 increased the minimum inhibitory concentration (MIC) of meropenem from 0.03 to 32 mg/L. Adding our inhibitors at a concentration of 500 μM resulted in a 32-64-fold reduction in the MIC of meropenem demonstrating that compounds **5αF** and **5αE** were potent synergists (Table 2). For comparison, L- and D-captopril displayed a 32-fold reduction in the MIC of

Table 1

Structures and inhibitory activities of trifluoromethyl mercaptopropionamide derivatives **5α(A-G)** and **5β(A-H)** against NDM-1.

Entry	Compound	Structure	IC$_{50}$ (μM)[a]
1	L-captopril		7 ± 2 (157[d])
2	*rac*-**5αA**		20 ± 2
3	(+)-**5αA**[b]		10 ± 3 (1.5[e])
4	(−)-**5αA**[b]		75 ± 15 (5[e])
5	**5βA**		>300
6	**5αB**		65 ± 14
7	**5βB**		>300
8	(2R,2'S)-**5αC**		4.5 ± 1.5 (64[d])
9	(2R,2'R)-**5αC**		0.3 ± 0.1 (20[d]/8[e]/22[f])
10	**5βC**		>300
11	mix-**5αD**[c]		37 ± 18
12	(2S,2'S)-**5αD**		60 ± 20 (>500[d])
13	(2S,2'R)-**5αD**		6.1 ± 1.6
14	**5βD**		>300
15	**5αE**		3.2 ± 0.7 (6.9[f])
16	**5βE**		145 ± 20
17	**5αF**		2.2 ± 0.5 (4.9[f])

Table 1 (*continued*)

Entry	Compound	Structure	IC$_{50}$ (μM)[a]
18	**5βF**		>300
19	**5αG**		3.4 ± 0.5
20	**5βG**		22 ± 6
21	**5βH**		5.6 ± 1.4

[a] The experiments were run in at least two parallel replicates, and the inhibitory activities are given as the mean value along with the standard error of the mean.
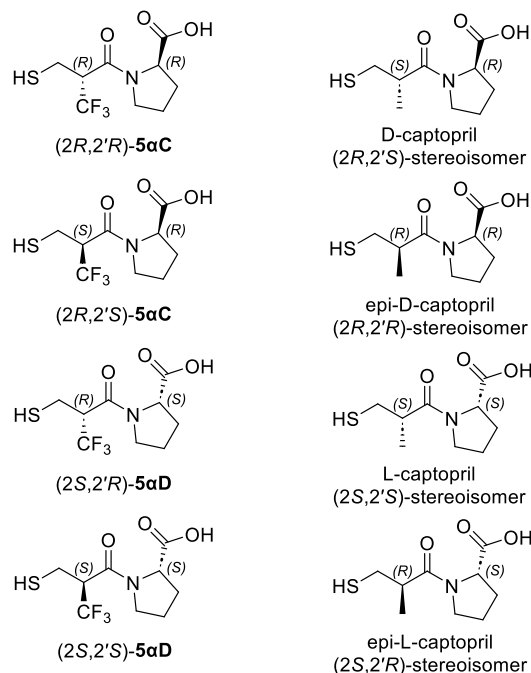
[b] Stereochemistry assigned based on docking and NMR results in accordance with [13b].

[c] Mixture of diastereomers (approximately 3:1 of (2S,2'S)-**5αD** to (2S,2'R)-**5αD**).

[d] Reported IC$_{50}$ values of non-fluorinated analogue in reference [14a].

[e] Reported IC$_{50}$ values of non-fluorinated analogue in reference [13b].

[f] Reported IC$_{50}$ value of non-fluorinated analogue in reference [13c].

Fig. 2. Captopril stereoisomers and their trifluoromethyl-containing analogues.

meropenem. The tested inhibitors in themselves did not affect bacterial growth at the used concentration (500 μM).

The most potent synergists against NDM-1 were further evaluated for their synergistic effect against the B1 MBLs VIM-2 and IMP-26 (Table 2) at a fixed concentration of 500 μM. The minimum inhibitory concentration of meropenem alone was 0.5 and 2 mg/L for VIM-2 and IMP-26, respectively. The most potent synergist (2S,2'R)-**5αD** showed an 8-fold reduction in the MIC of meropenem for both VIM-2 and IMP-26. L-captopril and its fluorinated analogue (2S,2'R)-**5αD** displayed the same synergistic activity against VIM-2 and IMP-26, while D-captopril showed stronger synergy than its fluorinated analogue (2R,2'R)-**5αC**.

Table 2

MIC of meropenem (MEM) in combination with selected inhibitors. Suscepti-bility was determined using *E. coli* E. cloni™ producing NDM-1, VIM-2 or IMP-26 from a low copy number plasmid [27].

Inhibitor	MIC meropenem (mg/L)[a,b]		
	MP30-63 *bla*NDM-1	MP30-57 *bla*VIM-2	MP30-58 *bla*IMP-26
No inhibitor control	32	0.5	2
D-captopril	1	0.06	0.5
L-captopril	1	0.06	0.25
(2R,2′R)-**5αC**	4	0.25	4
(2S,2′R)-**5αD**	4	0.06	0.25
5αF	1	0.125	2
5αE	0.5	0.125	0.5

[a] Minimal inhibitory concentration was tested in the presence of 500 μM of the inhibitor in duplicates.

[b] Meropenem MIC of *E. coli* E.cloni™ (MP21-05) without *bla* genes = 0.03 mg/L.

2.3. NMR determination of the binding pose

We isolated the enantiomers of rac-**5αA** using preparative chiral HPLC (for details see the Supporting Information) and characterized their binding to NDM-1 using solution-state NMR. A solution of uni-formly ^{15}N-enriched NDM-1, expressed and purified as described pre-viously [20b] and dissolved in 2.5 % DMSO in an aqueous KH_2PO_4 buffer, was titrated with (+)-**5αA** and (−)-**5αA** and the weighted chemical shift changes, $\Delta\delta_{1H,15N}$, of the backbone amide functionalities were recorded. ^{1}H,^{15}N HSQC spectra were acquired after addition of 0, 0.5, 1, 1.5, 3, 6, 10, and 15 equivalents of the two ligands. The last titration step was omitted for the quantification of the binding of (−)-**5αA** because of sample precipitation. Both enantiomers showed binding in the slow exchange regime, with the resonances of the free and the ligand-bound forms of the protein being simultaneously detectable, with varying intensities, throughout the titration. In accordance with literature [20b], we classified chemical shift perturbations (CSP, eq. (1), where R_{scale} = 6.5 [28]) as significant (SSP) when the observed $\Delta\delta_{1H,15N}$ was greater than the population mean plus the standard deviation (μ+1σ).

$$\text{CSP} = \Delta\delta_{(1H,15N)} = \sqrt{\left(\Delta\delta_{1H}{}^2 + \left(\frac{1}{R_{scale}} \times \Delta\delta_{15N}{}^2\right)\right)} \quad (1)$$

Significant chemical shift perturbations were observed for Thr119, His122, Asp124, Gly188, His189, Ser191, Lys211, Asp212, Ser213 Gly222, Thr226, Glu227, His228, Ser255, Lys268, Leu269, and Arg270 (Fig. 3), indicating that these amino acids either are involved in ligand binding or undergo larger binding induced conformational changes. These chemical shift perturbations were quantified (Table S3, Support-ing Information), providing the dissociation constant K_d 149.2 ± 21.8 μM for enantiomer (+)-**5αA** by fitting the binding induced signal in-tensity changes to eq. (2) [29].

$$I_{obs} = I_{max}\frac{([P] + [L] + K_d) - \sqrt{([P] + [L] + K_d)^2 - 4[P][L]}}{2[P]} \quad (2)$$

where K_d is the dissociation constant, I_{obs} are the normalized integrals of the protein-ligand complex, I_{max} is the normalized integral for the last titration step, and [P] and [L] are protein and ligand concentrations, respectively. The K_d was the average of the K_d values separately ob-tained for the amino acids showing SSP. Due to the weaker binding of enantiomer (−)-**5αA**, its K_d could not be estimated.

We obtained additional information on the binding pose of (+)-**5αA** by detection of ^{19}F,^{1}H heteronuclear Overhauser effects (HOEs) between its trifluoromethyl functionality and the protons of NDM-1. Amino acids Met67, His122 and Trp93 showed HOEs (Fig. 4), which corroborates the
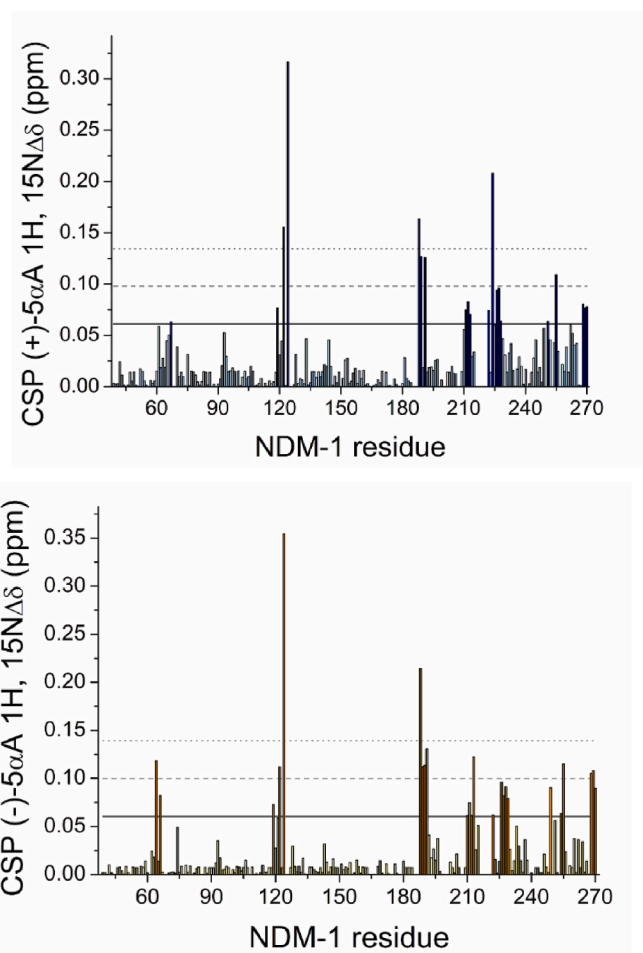

Fig. 3. The chemical shift perturbation (CSP) of the backbone amides of ^{15}N-labelled NDM-1 upon addition of 15 equivalents of (+)-**5αA** (upper) and (−)-**5αA** (lower). CSPs of residues above the first horizontal cut-off (solid line) are greater than the population mean plus standard deviation (μ+1σ), and are therefore considered to be significantly influenced by ligand binding. The solid and dashed lines represent the population mean (μ) plus one, two, and three standard deviations (σ), respectively.

large chemical shift perturbations observed for these amino acids during the titration experiment, indicating them to be directly involved in ligand binding.

2.4. Identification of the binding pose by molecular docking

Flexible docking of both enantiomers of **5αA** and of its previously known non-fluorinated analogue *N*-benzyl-3-mercapto-2-methyl-propanamide [13b] was performed using the software Glide followed by Prime (Schrödinger Inc.), starting from the NDM-1 crystal structure PDB:5ZIO [13c] and using the MM-GBSA rescoring protocol. The docking poses were filtered, removing those incompatible with the binding induced NMR chemical shifts shown in Fig. 3, and with the HOEs shown in Fig. 4. The predicted binding mode of (*R*)-*N*-benzyl-3--mercapto-2-methylpropanamide was in agreement with the X-ray structure 5ZIO [13c]. Conceivable binding poses were then ranked based on their binding energies, with the best ranked poses shown in Fig. 5. The binding poses of (*R*)-*N*-benzyl-3-mercapto-2-methylpropa-namide and of (+)-**5αA** possessed comparable binding energies, ΔG_{bind} = −58.68 kcal/mol and −58.45 kcal/mol, respectively, whereas the (−)-**5αA** enantiomer is predicted to bind significantly weaker to NDM-1 (ΔG_{bind} = −50.35 kcal/mol). This is in line with the experimentally determined IC$_{50}$ values of these compounds (1.5 μM for
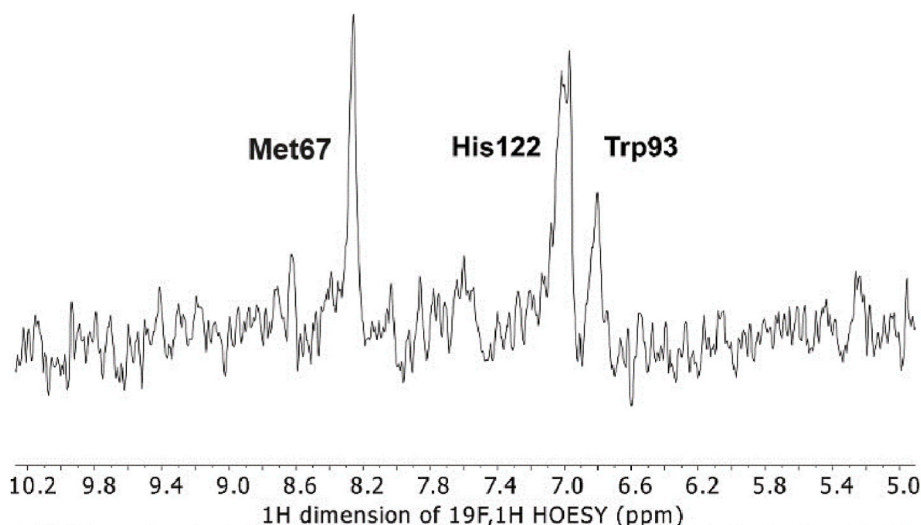
Fig. 4. Selective ^{19}F,^{1}H HOESY spectrum observed for the (+)-**5αA** - NDM-1 complex. Upon irradiation of the trifluoromethyl functionality, HOE was observed on the ^{1}H NMR signals of Met67 (8.26 ppm), His122 (7.01 ppm) and Trp93 (6.85 ppm). The interaction of NDM-1 (0.25 mM) and (+)-**5αA** (2.5 mM) was studied in a 20 mM KH$_2$PO$_4$ and 0.1 mM ZnCl$_2$ aqueous solutions (pH 7) on a 700 MHz NMR spectrometer, with irradiation at – 68.18 ppm (^{19}F NMR, CF$_3$).
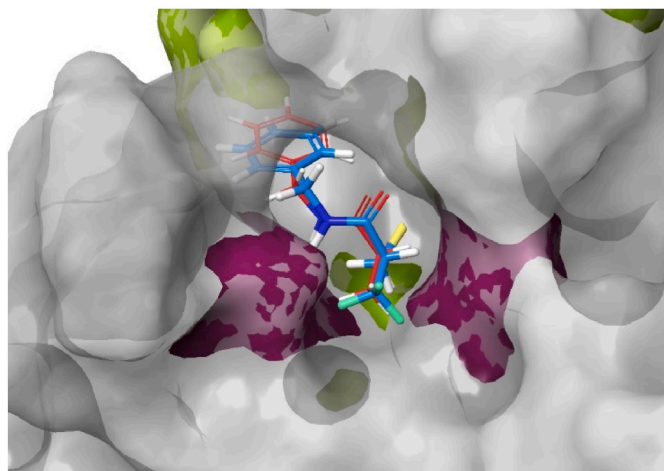
Fig. 5. The superimposed structures of (*R*)-*N*-benzyl-3-mercapto-2-methyl-propanamide (red) and (+)-**5αA** (blue) in complex with NDM-1, predicted by NMR-guided docking. Amino acids showing significant chemical shift perturbation upon ligand binding (SSP) are highlighted in green, and those showing HOE to the trifluoromethyl group of (+)-**5αA** in purple.

(*R*)-*N*-benzyl-3-mercapto-2-methylpropan–amide [13b], 10 μM (+)-**5αA** and 75 μM for (−)-**5αA**). Not just the binding energies, but even the binding modes of (*R*)-*N*-benzyl-3-mercapto-2-methylpropana-mide and (+)-**5αA** are highly similar. This suggests that fluorination did not considerably influence the binding pose of (*R*)-*N*-benzyl-3-mercap-to-2-methylpropanamide. Hence, both the native and the tri-fluoromethyl substituted inhibitors bind both zinc ions of the NDM-1 binding site via their thiol functionality (2.3 Å), and their carbonyl group forms a hydrogen bond with the side chain amide of Asn220 (1.6–1.7 Å). An N–H⋯F–C hydrogen bond (2.2 Å) was predicted be-tween the Gln123 amide proton of NDM-1 and the trifluoromethyl group of (+)-**5αA** that, however, is neither supported by an HOE correlation (NMR) nor by the inhibitory activity of (+)-**5αA** as compared to *N*-benzyl-3-mercapto-2-methylpropanamide. It should here be noted that our NMR data and energetic ranking based selection of theoretically feasible binding poses successfully identified the more active enan-tiomer, (+)-**5αA**, and allowed the determination of its binding pose, which well complements the data provided by Li et al. on the non-fluorinated analogue, *N*-benzyl-3-mercapto-2-methylpropanamide

[13b]. Due to the structural similarity of **5α(B–H)** and **5β(A-H)** to (+)-**5αA**, it is reasonable to presume that the compounds studied herein have comparable binding modes to NDM-1.

3. Conclusion

A series of novel trifluoromethylated captopril analogues was syn-thesized with several compounds demonstrating low-micromolar inhibitory activity against the B1 MBL NDM-1. The most active inhibi-tor was the CF$_3$-analogue of D-captopril with an IC$_{50}$ value of 0.3 μM. Derivatives with an α-CF$_3$ group proved to be by far more active against NDM-1 than β-CF$_3$–containing compounds, while exhibiting consider-ably lower stability towards oxidation. Substitution of the α-CH$_3$ group with an α-CF$_3$ group did not seem to significantly influence the inhibi-tory activity. Several of the α–CF$_3$–containing inhibitors were potent synergists, on the same level as L-captopril, and were able to repoten-tiate meropenem in NDM-1 (up to 64-fold), VIM-2 (up to 8-fold) and IMP-26 (up tp 8-fold) harbouring *E. coli*. Direct comparison of an α–CF$_3$–containing and non-fluorinated D- and L-captopril indicates that the fluorinated inhibitors are only slightly less potent synergists.

Using NMR spectroscopy and molecular docking the binding pose of one representative molecule with NDM-1 was identified. The binding pose of the fluorine-labelled inhibitor resembled the binding pose determined for the crystal structure of L-captopril with NDM-1, demonstrating that fluorine-labelled analogues of inhibitors are valu-able probes for the determination of binding poses.

In conclusion, trifluoromethylated captopril analogues are potent MBL inhibitors and, thus, can become promising tools for structural studies of MBL-binding poses.

4. Experimental section

Description of the experimental procedures can be found in the Supporting information. Biological activity raw data will be made available through the DataverseNO repository before publication. The backbone resonance assignment [20b] of NDM-1 was deposited to the BMRBI with code 50945.

CRediT authorship contribution statement

Alexandra Kondratieva: Conceptualization, Data curation, Formal analysis, Investigation, Methodology, Software, Validation,

Visualization, Writing – original draft, Writing – review & editing. **Katarzyna Palica:** Formal analysis, Investigation, Methodology, Software, Validation, Visualization, Writing – original draft. **Christopher Frøhlich:** Investigation, Methodology, Supervision, Visualization, Writing – original draft, Writing – review & editing. **Rebekka Rolfsnes Hovd:** Methodology, Writing – review & editing. **Hanna-Kirsti S. Leiros:** Funding acquisition, Supervision, Writing – original draft, Writing – review & editing. **Mate Erdelyi:** Conceptualization, Funding acquisition, Methodology, Resources, Supervision, Writing – original draft, Writing – review & editing. **Annette Bayer:** Conceptualization, Funding acquisition, Methodology, Project administration, Resources, Supervision, Writing – original draft, Writing – review & editing.

Declaration of competing interest

The authors declare that they have no known competing financial interests or personal relationships that could have appeared to influence the work reported in this paper.

Data availability

Supporting information for compound identity and purity are attached as Supporting information. Biological data will be made available on request.

Acknowledgements

Appendix A. Supplementary data

Supplementary data to this article can be found online at https://doi.org/10.1016/j.ejmech.2024.116140.

References

[1] WHO in *Global action plan on Antimicrobial resistance*, Vol. Geneva, 2015.
[2] a) T. Palzkill, Ann. N. Y. Acad. Sci. 1277 (2013) 91–104;
    b) J.D. Docquier, S. Mangani, Drug Resist. Updates 36 (2018) 13–29.
[3] K. Bush, G.A. Jacoby, Antimicrob. Agents Chemother. 54 (2010) 969–976.
[4] T. Naas, S. Oueslati, R.A. Bonnin, M.L. Dabos, A. Zavala, L. Dortet, P. Retailleau, B. I. Iorga, J. Enzym. Inhib. Med. Chem. 32 (2017) 917–919.
[5] a) N. Farhat, A.U. Khan, Infect. Genet. Evol. 86 (2020) 104588;
    b) G. Bahr, L.J. González, A.J. Vila, Chem. Rev. 121 (2021) 7957–8094.
[6] D. Yahav, C.G. Giske, A. Grämatniece, H. Abodakpi, V.H. Tam, L. Leibovici, Clin. Microbiol. Rev. 34 (2020), https://doi.org/10.1128/cmr.00115-20 e00115-00120.
[7] a) M.F. Mojica, M.A. Rossi, A.J. Vila, R.A. Bonomo, Lancet Infect. Dis. 22 (2022) e28–e34;
    b) E. Denakpo, T. Naas, B.I. Iorga, Expert Opin. Ther. Pat. (2023) 1–16;
    c) X. Gu, M. Zheng, L. Chen, H. Li, Microbiol. Res. 261 (2022) 127079.
[8] a) P. Linciano, L. Cendron, E. Gianquinto, F. Spyrakis, D. Tondi, ACS Infect. Dis. 5 (2019) 9–34;
    b) Y. Yang, Y.-H. Yan, C.J. Schofield, A. McNally, Z. Zong, G.-B. Li, Trends Microbiol. 31 (2023) 735–748.
[9] a) K. Bush, P.A. Bradford, Nat. Rev. Microbiol. 17 (2019) 295–306;
    b) K.H.M.E. Tehrani, N.I. Martin, Med. Chem. Commun. 9 (2018) 1439–1456.
[10] a) Y.L. Wang, S. Liu, Z.J. Yu, Y. Lei, M.Y. Huang, Y.H. Yan, Q. Ma, Y. Zheng, H. Deng, Y. Sun, C. Wu, Y. Yu, Q. Chen, Z. Wang, Y. Wu, G.B. Li, J. Med. Chem. 62 (2019) 7160–7184;
    b) S. Yahiaoui, K. Voos, J. Haupenthal, T.A. Wichelhaus, D. Frank, L. Weizel, M. Rotter, S. Brunst, J.S. Kramer, E. Proschak, C. Ducho, A.K.H. Hirsch, RSC Med. Chem. 12 (2021) 1698–1708;
    c) Y.H. Yan, J. Chen, Z. Zhan, Z.J. Yu, G. Li, L. Guo, G.B. Li, Y. Wu, Y. Zheng, RSC Adv. 10 (2020) 31377–31384;
    d) Z. Meng, M.L. Tang, L. Yu, Y. Liang, J. Han, C. Zhang, F. Hu, J.M. Yu, X. Sun, ACS Infect. Dis. 5 (2019) 903–916;
    e) F.M. Klingler, T.A. Wichelhaus, D. Frank, J. Cuesta-Bernal, J. El-Delik, H. F. Muller, H. Sjuts, S. Gottig, A. Koenigs, K.M. Pos, D. Pogoryelov, E. Proschak, J. Med. Chem. 58 (2015) 3626–3630.
[11] D.W. Cushman, M.A. Ondetti, Nat. Med. 5 (1999) 1110–1112.
[12] a) Y. Yusof, D.T.C. Tan, O.K. Arjomandi, G. Schenk, R.P. McGeary, Bioorg. Med. Chem. Lett. 26 (2016) 1589–1593;
    b) B.M. Lienard, G. Garau, L. Horsfall, A.I. Karsisiotis, C. Damblon, P. Lassaux, C. Papamicael, G.C. Roberts, M. Galleni, O. Dideberg, J.M. Frere, C.J. Schofield, Org. Biomol. Chem. 6 (2008) 2282–2294;
    c) U. Heinz, R. Bauer, S. Wommer, W. Meyer-Klaucke, C. Papamichaels, J. Bateson, H.W. Adolph, J. Biol. Chem. 278 (2003) 20659–20666.
[13] a) C. Kaya, J. Konstantinović, A.M. Kany, A. Andreas, J.S. Kramer, S. Brunst, L. Weizel, M.J. Rotter, D. Frank, S. Yahiaoui, R. Müller, R.W. Hartmann, J. Haupenthal, E. Proschak, T.A. Wichelhaus, A.K.H. Hirsch, J. Med. Chem. 65 (2022) 3913–3922;
    b) N. Li, Y. Xu, Q. Xia, C. Bai, T. Wang, L. Wang, D. He, N. Xie, L. Li, J. Wang, H. G. Zhou, F. Xu, C. Yang, Q. Zhang, Z. Yin, Y. Guo, Y. Chen, Bioorg. Med. Chem. Lett. 24 (2014) 386–389;
    c) G. Ma, S. Wang, K. Wu, W. Zhang, A. Ahmad, Q. Hao, X. Lei, H. Zhang, Bioorg. Med. Chem. 29 (2021) 115902.
[14] a) J. Brem, S.S. van Berkel, D. Zollman, S.Y. Lee, O. Gileadi, P.J. McHugh, T. R. Walsh, M.A. McDonough, C.J. Schofield, Antimicrob. Agents Chemother. 60 (2016) 142–150;
    b) Y. Guo, J. Wang, G. Niu, W. Shui, Y. Sun, H. Zhou, Y. Zhang, C. Yang, Z. Lou, Z. Rao, Protein Cell 2 (2011) 384–394.
[15] a) A.M. Rydzik, J. Brem, S.S. van Berkel, I. Pfeffer, A. Makena, T.D.W. Claridge, C. J. Schofield, Angew. Chem. Int. Ed. 53 (2014) 3129–3133;
    b) S.S. van Berkel, J. Brem, A.M. Rydzik, R. Salimraj, R. Cain, A. Verma, R. J. Owens, C.W.G. Fishwick, J. Spencer, C.J. Schofield, J. Med. Chem. 56 (2013) 6945–6953.
[16] a) C. Mollard, C. Moali, C. Papamicael, C. Damblon, S. Vessilier, G. Amicosante, C. J. Schofield, M. Galleni, J.M. Frère, G.C.K. Roberts, J. Biol. Chem. 276 (2001) 45015–45023;
    b) K.H.M.E. Tehrani, N.I. Martin, ACS Infect. Dis. 3 (2017) 711–717.
[17] K.H.M.E. Tehrani, N. Wade, V. Mashayekhi, N.C. Bruchle, W. Jespers, K. Voskuil, D. Pesce, M.J. van Haren, G.J.P. van Westen, N.I. Martin, J. Med. Chem. 64 (2021) 9141–9151.
[18] a) A. Abula, Z. Xu, Z. Zhu, C. Peng, Z. Chen, W. Zhu, H.A. Aisa, J. Chem. Inf. Model. 60 (2020) 6242–6250;
    b) B.M. Johnson, Y.-Z. Shu, X. Zhuo, N.A. Meanwell, J. Med. Chem. 63 (2020) 6315–6386;
    c) N.A. Meanwell, J. Med. Chem. 61 (2018) 5822–5880.
[19] a) I. Ojima, F.A. Jameison, B. Pete, H. Radunz, C. Schittenhelm, H.J. Linder, A. E. Emith, Drug Des. Discov. 11 (1994) 91–113;
    b) I. Ojima, F.A. Jameison, Bioorg. Med. Chem. Lett. 1 (1991) 581–584.
[20] a) G. Rivière, S. Oueslati, M. Gayral, J.B. Créchet, N. Nhiri, E. Lescop, J. C. Cintrat, F. Giraud, C. van Heijenoort, E. Lescop, S. Pethe, B.I. Iorga, T. Naas, E. Guittet, N. Morellet, ACS Omega 5 (2020) 10466–10480;
    b) K. Palica, M. Vorácová, S. Skagseth, A. Andersson Rasmussen, L. Allander, M. Hubert, L. Sandegren, H.-K.S. Leiros, H. Andersson, M. Erdélyi, ACS Omega 7 (2022) 4550–4562;
    c) K. Cheng, Q. Wu, C. Yao, Z. Chai, L. Jiang, M. Liu, C. Li, JACS Au 3 (2023) 849–859;
    d) L.H.E. Wieske, J. Bogaerts, A.A.M. Leding, S. Wilcox, A. Andersson Rasmussen, K. Leszczak, L. Turunen, W.A. Herrebout, M. Hubert, A. Bayer, M. Erdélyi, ACS Med. Chem. Lett. 13 (2022) 257–261.
[21] Y. Hu, K. Cheng, L. He, X. Zhang, B. Jiang, L. Jiang, C. Li, G. Wang, Y. Yang, M. Liu, Anal. Chem. 93 (2021) 1866–1879.
[22] R.S. Norton, E.W.W. Leung, I.R. Chandrashekaran, C.A. MacRaild, Molecules 21 (2016) 860–873.
[23] E. van Groesen, C.T. Lohans, J. Brem, K.M.J. Aertker, T.D.W. Claridge, C. J. Schofield, Chem. Eur J. 25 (2019) 11837–11841.
[24] T.P. Vasilева, A.F. Kolomiets, E.I. Mysov, A.V. Fokin, Russ. Chem. Bull. 46 (1997) 1230–1232.
[25] S. Skagseth, S. Akhter, M.H. Paulsen, Z. Muhammad, S. Lauksund, Ø. Samuelsen, H.-K.S. Leiros, A. Bayer, Eur. J. Med. Chem. 135 (2017) 159–173.
[26] D. Buttner, J.S. Kramer, F.M. Klingler, S.K. Wittmann, M.R. Hartmann, C.G. Kurz, D. Kohnhauser, L. Weizel, A. Bruggerhoff, D. Frank, D. Steinhilber, T. A. Wichelhaus, D. Pogoryelov, E. Proschak, ACS Infect. Dis. 4 (2018) 360–372.
[27] a) C. Fröhlich, V. Sørum, N. Tokuriki, P.J. Johnsen, Ø. Samuelsen, J. Antimicrob. Chemother. 77 (2022) 2429–2436;
    b) Ø.M. Lorentzen, A.S.B. Haukefer, P.J. Johnsen, C. Frøhlich, bioRxiv (2023), 2023.2010.2002.560492.
[28] M.P. Williamson, Prog. Nucl. Magn. Reson. Spectrosc. 73 (2013) 1–16.
[29] L. Fielding, Curr. Top. Med. Chem. 3 (2003) 39–53.